V44

X-ray Reflectrometry

Jonas Ollesch
jonas.ollesch@tu-dortmund.de

Lukas Annuss
lukas.annuss@tu-dortmund.de

Excution: 29.01.2024

Hand-In: 09.02.2024

TU Dortmund – Fakultät Physik

Contents

1 Objective

This experiment's objective is to measure the density, roughness and layer thickness of a polysterol film on a silicon wafer as well as the dispersion and roughness of the wafer itself through the use X-ray reflectrometry.

2 Theory

To reasonably discuss the experiment's execution as well as later evaluate the measurements, some theoretical basics are needed.

2.1 X-rays

The term X-ray describes electromagnetic radiation with an energy of around 1 keV to 100 keV [1]. As shown in Figure 1, one possibility of producing such radiation is through the use of an X-ray tube.

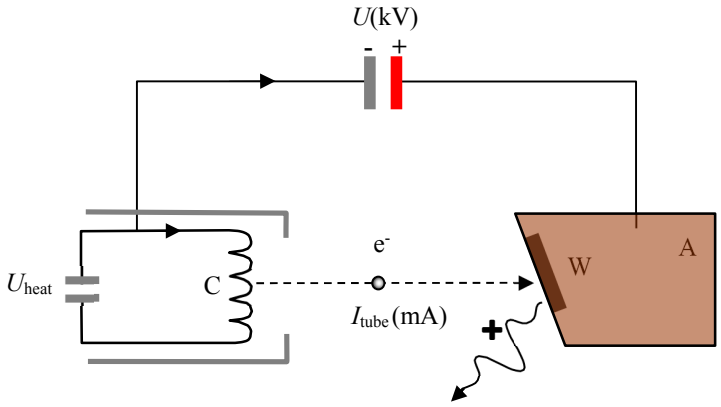

Figure 1: Schematic view of an X-ray tube with cathode C and anode A [2].

A wire is heated by a voltage U_{heat} until it becomes incandescent. Thus, it emits electrons, which are then accelerated towards the anode through a high voltage between cathode C and anode A. When they hit the anode material, they lose energy through interaction, namely through bremsstrahlung and ionisation. Bremsstrahlung describes radiation that is emitted when electrons interact with the Coulomb field of an atomic nucleus and lose energy in the form of photons. Ionisation happens if the incoming electron hits another electron inside the anode and transfers enough energy for the anode electron to leave its atom. The free space inside the atomic shell is then refilled by electrons of higher energy levels which in turn emit their energy in the form of photons. These photons posses exactly the energy between the levels, so

$$E_\gamma = \Delta E = E' - E$$

for energy level E' on the higher and energy E on the lower level. This means that the characteristic spectrum and thus the photon energy is dependent on the anode material

since different materials posses different binding energies. Approximately,

$$E_n \propto \frac{Z^2}{n^2}$$

holds for the energy of level n with atomic number Z. While bremsstrahlung is emitted as a continuous spectrum, the X-rays created by ionisation posses a characteristic and discrete wavelength depending on the energy level of the ionised electron as seen in Figure 2.

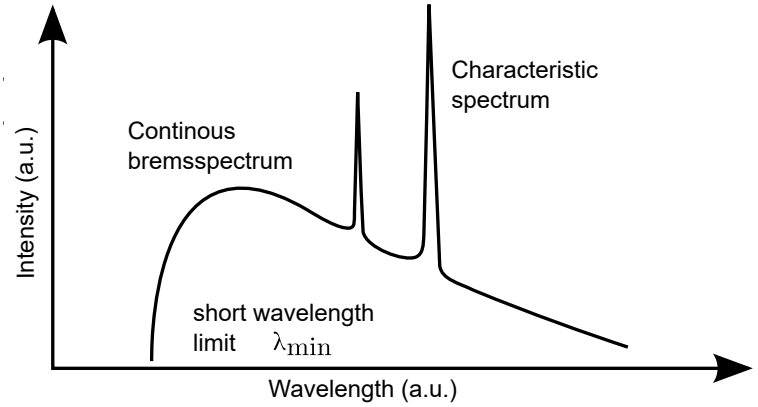

Figure 2: Schematic view of the X-ray spectrum of a material showing the continuous spectrum of the bremsstrahlung as well as the characteristic peaks for ionisation [3].

It can also be seen that the bremsspectrum only begins at a certain wavelength $\lambda_{\min}$. This wavelength can be derived from

$$E = hf = \frac{hc}{\lambda}$$

to be

$$\lambda_{\min} = \frac{hc}{eU_{\mathrm{A}}}$$

with energy E, frequency f, the Planck constant h, light speed c, elementary charge e and acceleration voltage U_{A}.

X-rays behave differently when passing through and being reflected by different materials.

2.2 Single-interface Refraction

When hitting a single flat surface, the refractive index for X-rays can be described by

$$n = 1 - \delta + i\beta\,. \tag{1}$$

The terms

$$\delta(r) = \frac{\lambda^2}{2\pi} r_\mathrm{e} \rho(r) \sum_{j=1}^{N} \frac{f_j^0 + f_j'}{Z}$$

and

$$\beta(r) = \frac{\lambda^2}{2\pi} r_\mathrm{e} \rho(r) \sum_{j=1}^{N} \frac{f_j''}{Z} = \frac{\lambda}{4\pi} \mu(r)$$

describe a dispersion an absorption term with $\delta > 0$ and $\beta \propto \mu(r)$ where $\mu(r)$ is the linear absorption coefficient, where $f_j = f_j^0 + f_j'(E) + i f_j''(E)$ describes forced oscillation strengths with dispersion and absorption corrections f_j' and f_j''. The classical electron radius is denoted by r_e and the electron density is given by $\rho(r)$ with electron number Z [4].
The process of refraction and reflection is shown in Figure 3.

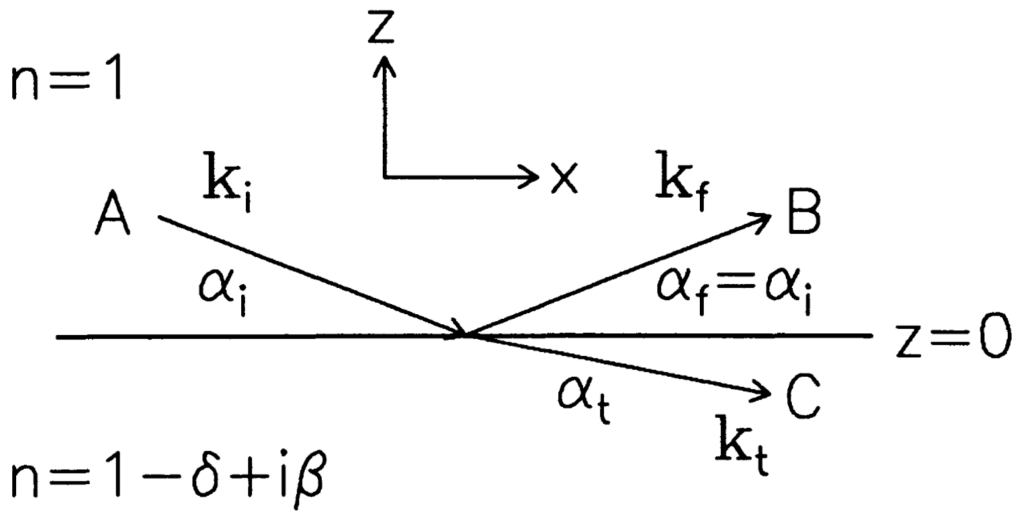

Figure 3: Refraction and reflection of a plane electromagnetic wave on a flat surface with grazing angle α_i, reflection angle $\alpha_\mathrm{f} = \alpha_\mathrm{i}$, transmission angle α_t and incoming, transmitted and reflected wave vectors k_i, k_t and k_f [4].

With $\delta \sim 10^{-6}$ and $\beta \sim 10^{-7}$ it can be seen that $|n| < 1$, although it may still be close to 1. This means that, for angles below a critical angle α_c, total reflection is possible. Assuming the exit angle α_t of the refracted beam to be zero, the critical angle is given by

$$\alpha_\mathrm{c} \approx \sqrt{2\delta} = \lambda \sqrt{\frac{r_\mathrm{e}\rho}{\pi}}\,, \tag{2}$$

where r_e is the classical electron radius, ρ the electron density and λ the wavelength of the X-ray photon [4].

In order to now describe the amplitude of transmitted and reflected X-rays, we use the Fresnel equations. Normally, for different polarisations of photons, different equations

apply. But here, since the refractive indices n_1 and n_2 of the vacuum and medium are almost identical (with corrections at $\mathcal{O}(10^{-6})$), the different equations are identical. For the reflected amplitude,

$$r = \frac{n_1 \cos\alpha_1 - n_2 \cos\alpha_2}{n_1 \cos\alpha_1 + n_2 \cos\alpha_2} \tag{3}$$

holds while the transmitted amplitude is described by

$$t = \frac{2n_1}{n_1 \cos\alpha_1 + n_2 \cos\alpha_2} \,. \tag{4}$$

The angles α_1 and α_2 describe the angles of the reflected and namely transmitted light.

These formulae allow us to calculate the so-called Fresnel reflectivity $R_\mathrm{F} = |r|^2$, which becomes

$$R_\mathrm{F} \simeq \left(\frac{\alpha_\mathrm{c}}{2\alpha_i}\right)^4 \tag{5}$$

for incident angles $\alpha_i > 3\alpha_\mathrm{c}$ [4]. For angles smaller than the critical angle, the Fresnel reflectivity is of $\mathcal{O}(1)$, then quickly drops at $\frac{\alpha_\mathrm{i}}{\alpha_\mathrm{c}} = 1$ and converges against zero for $\frac{\alpha_\mathrm{i}}{\alpha_\mathrm{c}} > 1$, comparable to the Fermi-Dirac-distribution for electrons.

2.3 Multi-interface Refraction

Until now, we have only looked at refraction of X-rays on a single interface surface. If the X-ray, or any electromagnetic radiation, instead hits a layered system, as seen in Figure 4, the radiation is refracted and transmitted at every single layer.

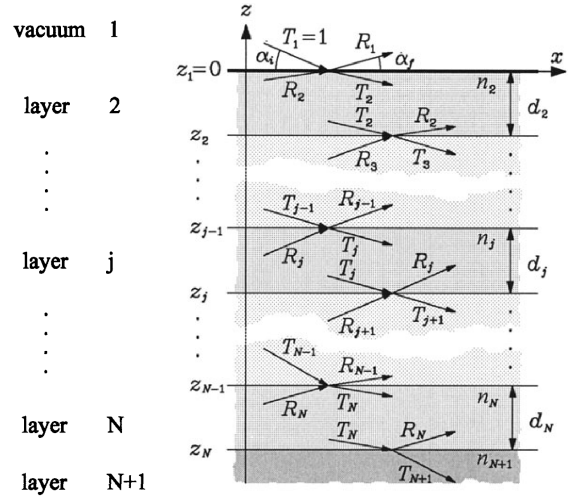

Figure 4: Refraction and reflection of a plane electromagnetic wave inside a $N+1$-layered system [4].

This also means that the transmitted rays from one layer can interfere with the reflected radiation from a deeper layer, causing oscillations in the systems reflectivity. These so-called *Kiessig oscillations* are shown in Figure 5 and in turn can be used to calculate the layer thickness. With the z-component of the wave vector transfer $q = \vec{k}_\mathrm{f} - \vec{k}_\mathrm{i}$, $q_\mathrm{z} = 2k \sin \alpha_i$, the layer thickness is

$$d = \frac{2\pi}{\Delta q_\mathrm{z}} \approx \frac{\lambda}{2\Delta\alpha_i} \,. \tag{6}$$

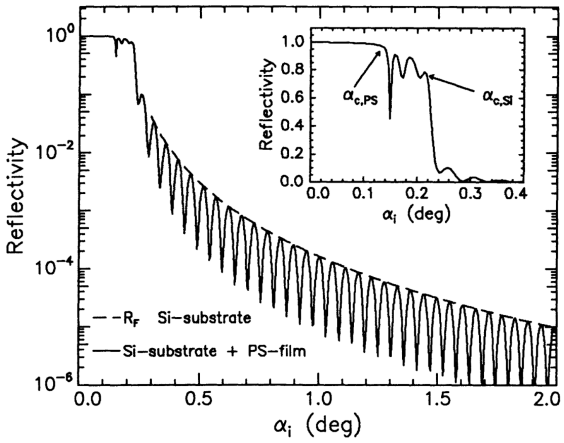

Figure 5: Graphic representation of Kiessig oscillations inside a multi-layered system with critical angles shown for polystyrene (PS) film and Si [4].

To calculate the Kiessig oscillations, the lowest layer is taken as a layer with infinite thickness without reflection from below, meaning $R_{N+1} = X_{N+1} = 0$. The rest of the layers is then recursively calculated from the bottom up, giving the recursive formula

$$X_j = \frac{R_j}{T_j} = \exp(-2ik_{z,j}z_j)\frac{r_{j,j+1} + X_{j+1}\exp(2ik_{z,j+1}z_j)}{1 + r_{j,j+1}X_{j+1}\exp(2ik_{z,j+1}z_j)} \,, \tag{7}$$

where

$$r_{j,j+1} = \frac{k_{z,j} - k_{z,j+1}}{k_{z,j} + k_{z,j+1}}$$

is the Fresnel coefficient of the j-th interface [4]. This approach is called *Parratt algorithm*.

2.4 Rough Surfaces

Real surfaces are seldom even. So we take an ensemble of even surfaces to approximate the rough surface as seen in Figure 6 and modify the Fresnel coefficient so that

$$\tilde{r}_{j,j+1} = r_{j,j+1}\exp(-2k_{z,j}k_{z,j+1}\sigma_j^2) \,, \tag{8}$$

where

$$\sigma^2 = \int (z - \mu_j)P_j(z)\mathrm{d}z = \int (z - z_j)P_j(z)\mathrm{d}z$$

is the root-mean-square roughness for a probability distribution P_j, here a Gaussian with mean $\mu_j = z_j$.

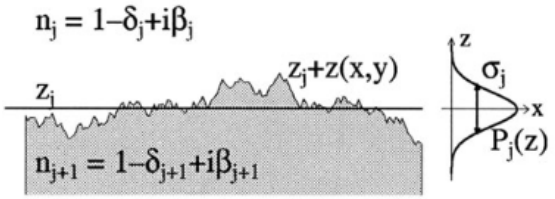

Figure 6: Schematic representation of a rough surface approximated by even surfaces at height $z + z_j$ with probability distribution P_j [4].

It should be noted that this modification works only for systems where the roughness σ_j is much smaller than the layer thickness d_j. For systems with greater roughness, the smaller even surfaces must be treated as different layers with their own refractive indices etc. [4].

2.5 Geometry Factor

It must also be noted that the beam used in this experiment still has a width b_i. Especially for small angles, it will cover more are than the sample with width D (shown in Figure 7), which has to be corrected by

$$G = \begin{cases} \frac{D \sin \alpha_\mathrm{i}}{d_0} & , \quad \alpha_\mathrm{i} < \alpha_\mathrm{g} \\ 1 & , \quad \alpha_\mathrm{i} > \alpha_\mathrm{g} \end{cases} \tag{9}$$

with total beam width d_0 and effective beam area $D \sin \alpha_\mathrm{i}$ [5].

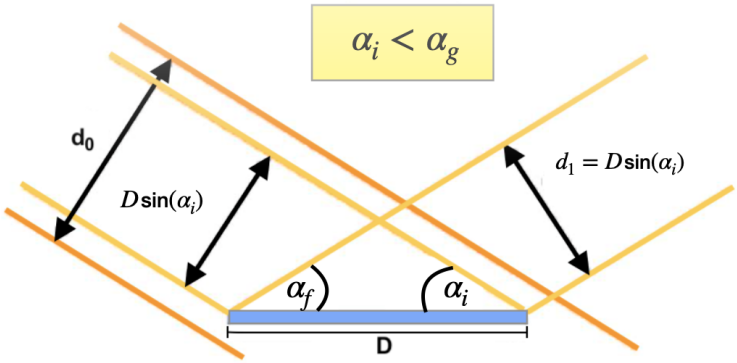

Figure 7: Schematic view at the beam hitting the sample at a low angle α_i where the beam area is larger than that of the sample [5].

3 Execution

A picture of the setup can be seen in Figure 8.

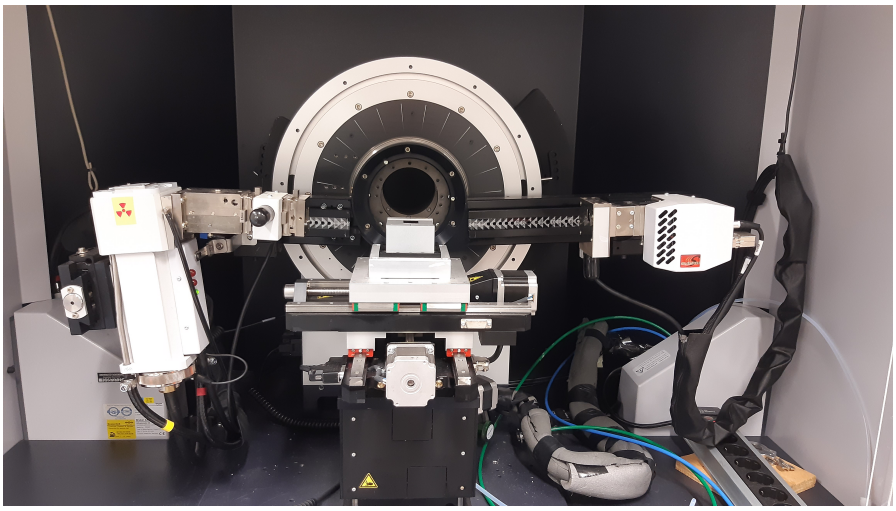

Figure 8: A photograph of the setup used in this experiment. On the left is the X-ray source and on the right the detector with the sample in the middle.

To perform the experiment, a D8 laboratory diffractometer from Bruker-AXS is used. The measurements themselves as well as drive control is being taken care of by the software XRD Command. As explained, the X-rays are created in an X-ray tube and then hit the Göbel mirror, a mirror specifically created to parallelise X-rays, since the tube emits them evenly throughout every direction. Then, the X-rays hit the sample and are reflected so that they can enter the detector.

This arrangement, however, has to be adjusted before the real measurement can be started. In order to do that, a multitude of scans is performed as shown in Figure 9.

Type	Range	Step size	Measuring time per mesuring point [s]
Detector scan	-0.5 to 0.5	0.02	1
Z-Scan	-1 to 1	0.04	1
X-Scan	-20 to 20	1	1
Rockingscan $2\theta = 0$	-1 to 1	0.04	1
Z-Scan	-0.5 to 0.5	0.02	1
Rockingscan $2\theta = 0.3$	0 to 0.3	0.005	1
Z-Scan $2\theta = 0.3$	-0.5 to 0.5	0.02	1
Rockingscan $2\theta = 0.5$	0.2 to 0.5	0.005	1

Figure 9: A table showing the different scans that have to be performed in order to align the sample and the detector, including the recommended settings for XRD Command [5].

As can be seen from the number of scans that need to be performed, it is important that the sample is aligned just right with the detector. Before beginning the sample alignment, the primary beam is adjusted. To do that, the sample is moved out of the beam by changing the z-coordinate and a detector scan is performed. This moves the detector in a small angular range, yielding a scan in the form of a Gaussian. the Gaussian's maximum is then chosen to be the new zero position of the detector.
Now, the sample alignment can begin. The z-coordinate is aligned by moving the sample through the X-ray until it blocks half the intensity. When adjusting the x-coordinate a plateau should show in the X-Scan. The middle of the plateau is chosen and the sample is moved there via the diffractometer's drives. After that, a Rockingscan is performed to adjust the y-coordinate, which, as well as the Z-Scan, is performed multiple times at different angles to ensure high precision. The Rockingscan gives information about the tilt of the sample relative to the X-ray beam. A correctly performed Rockingscan should yield a symmetrical triangle. This means that both the z-coordinate is aligned properly and that the sample is hit directly in its center of rotation of the diffractometer.

After the alignment, the measurements are performed. First, an **Omega/2Theta**-type scan with a range of 0° to 2.5° and a step size of 0.005° with 5 s per step is performed. Then, to measure the diffuse background, the detector is tilted by 0.2° and the same measurement is performed again.

4 Evaluation

The following regressions are performed with the method *curve_fit* from the python [6] package *scipy* [7]. Propagation of the uncertainties are done with the package *uncertainties* [8]. Plots are created with *matplotlib* [9].

4.1 Alignment

4.1.1 Detector scan

To adjust the primary beam a detector scan is performed. The recorded data and the Gaussian fit are depicted in Figure 10. The resulting reflectivity should represent a Gaussian distribution of the shape

$$R(\alpha) = \frac{a}{\sqrt{2\pi\sigma^2}} \cdot e^{-\frac{(x-\mu)^2}{2\sigma^2}} + b\,.$$

The parameter a, b, μ and σ are determined as

$$\begin{aligned} a &= (118\,153.296 \pm 0.070)^\circ\,, \\ b &= 11\,647.81 \pm 0.16\,, \\ \mu &= (-0.108\,711\,7 \pm 0.000\,002\,3)^\circ \quad \text{and} \\ \sigma &= (3.706\,477\,0 \pm 0.000\,002\,4)^\circ\,. \end{aligned}$$

The FWHM and the maximum of the reflectivity I_{max} are established as

$$\text{FWHM} = (0.087\,280\,89 \pm 0.000\,000\,06)^\circ \quad \text{and}$$
$$I_{\text{max}} = 1\,283\,375.91 \pm 0.68\,.$$

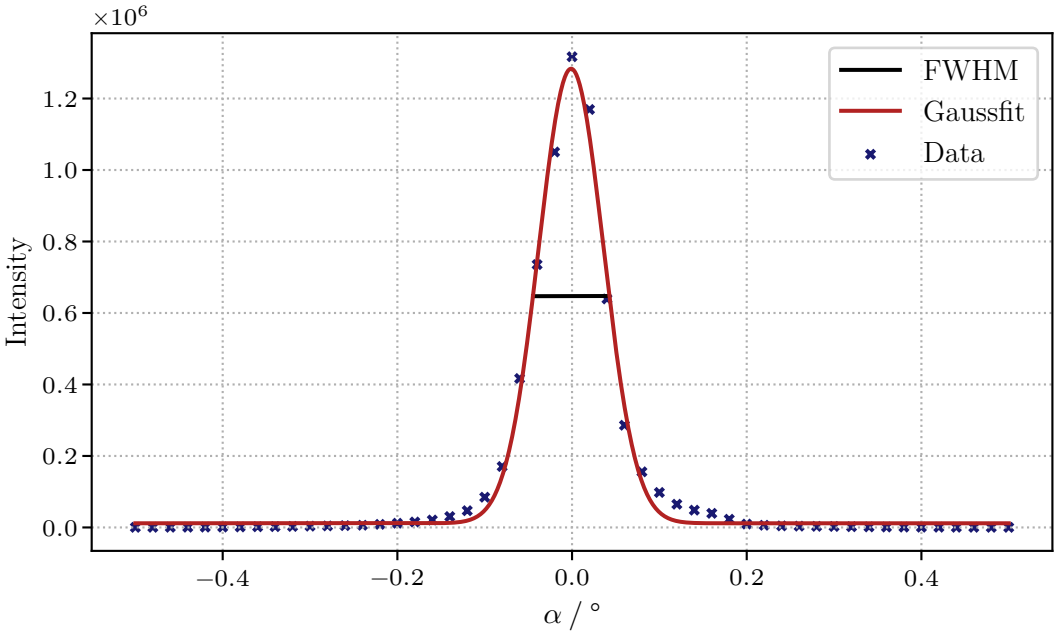

Figure 10: The intensity of the detector scan in dependence on the incidence angle $\alpha\,/\,^\circ$.

4.1.2 Z-Scan

During the Z-scan, the z-position of the sample is changed. The sample is moved from below into the primary beam until it is completely blocked, reducing the reflectivity to nearly zero. This measurement is shown in Figure 11. The width of the beam is

$$d_0 = (0.20 \pm 0.02)\,\text{mm}.$$

The uncertainty of the width is the distance between two measurement point.

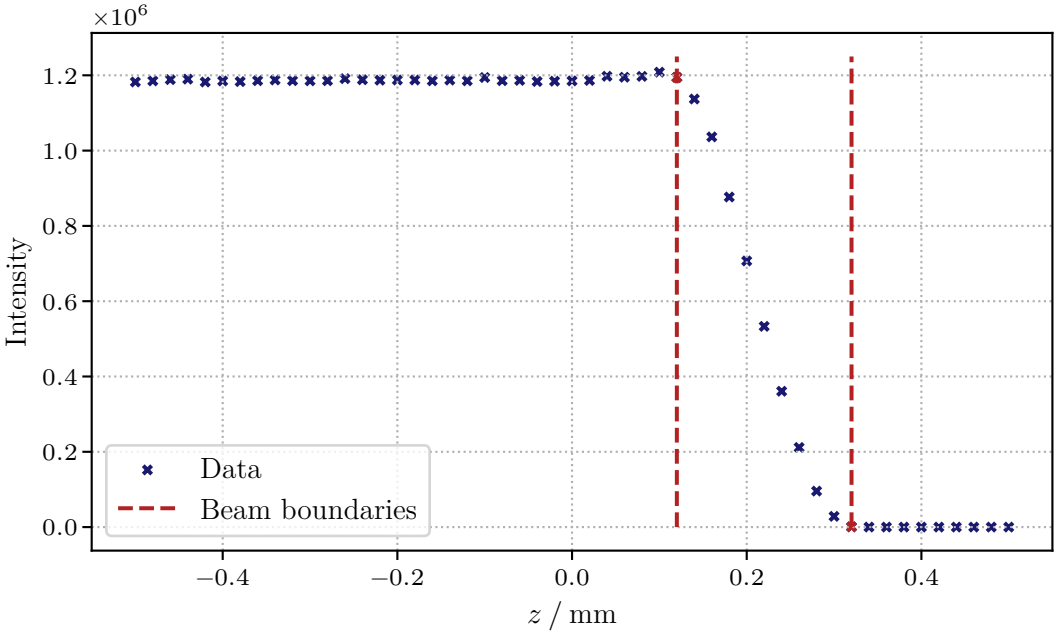

Figure 11: The measurement intensity for different positions of the probe. In addition the width of the beam is included.

4.1.3 Rockingscan

A Rockingscan is used to determine the geometry angle α_g. For this, the Figure 12 is evaluated, where α_g is half the base of the triangle. In this measurement α_g is measured as

$$\alpha_g = (0.520 \pm 0.020)^\circ = (0.009\,08 \pm 0.000\,35)\,\text{rad}\,.$$

Together with the width of the sample $D = 20.00\,\text{mm}$ [5], the width of the beam from subsubsection 4.1.2 and Equation 9 the theoretical value is calculated to be

$$\alpha_{\text{Theo}} = (0.573 \pm 0.057)^\circ = (0.0100 \pm 0.0010)\,\text{rad}\,.$$

For these angles the geometry factor is calculate, which results in

$$\text{G}_g = 0.0158 \pm 0.0017$$

and

$$\text{G}_{\text{Theo}} = 0.017\,453\,58 \pm 0.000\,000\,06\,.$$

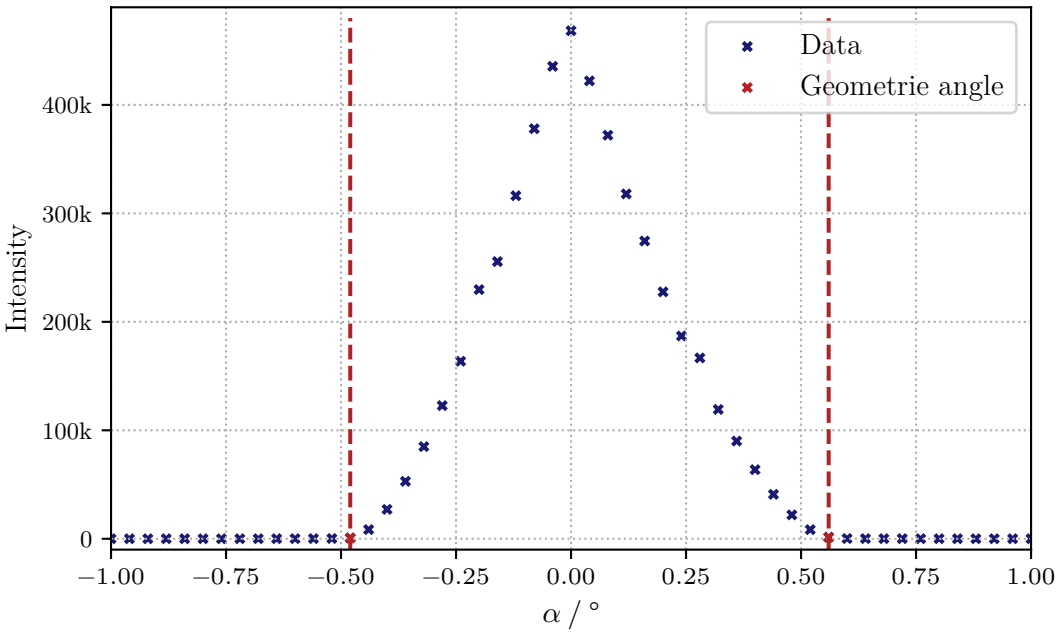

Figure 12: Intensity of the Rockingscan with $2\alpha = 0$ and the corresponding geometry angle.

4.2 Omega/2Theta

The setup records data for 5.00 s. To gain the true reflectivity the diffuse reflectivity is subtracted from the compact scan and modified by

$$R(I) = \frac{I}{5 \cdot I_{\max}} .$$

The factor 5 is included because the maximum intensity is only measured for 1.00 s. The true reflectivity is plotted in Figure 13 along with the background scan. In the following the measurement data is corrected by the measured geometry factor and is plotted in Figure 14. The Figure 15 shows the fit of the Parratt algorithm to the true reflectivity. As a comparison, the ideal reflectivity that the pure silicon wafer would produce is included. To determine this the layer thickness is calculate via Equation 6 and its value is

$$d = (8.8 \pm 0.7) \times 10^{-8}\,\mathrm{m} .$$

The best fit of the Parratt algorithm is achieved with *iminuit* [10]. The parameters are in Table 1.

Table 1: Best parameters established by fitting the Parratt algorithm.

Layer thickness	$8.49 \times 10^{-8}\,\mathrm{m}$
δ_{Si}	6.93×10^{-6}
δ_{Poly}	9.70×10^{-7}
β_{Si}	1.73×10^{-7}
β_{Poly}	4.85×10^{-9}
σ_{Si}	$7.90 \times 10^{-10}\,\mathrm{m}$
σ_{Poly}	$6.17 \times 10^{-10}\,\mathrm{m}$

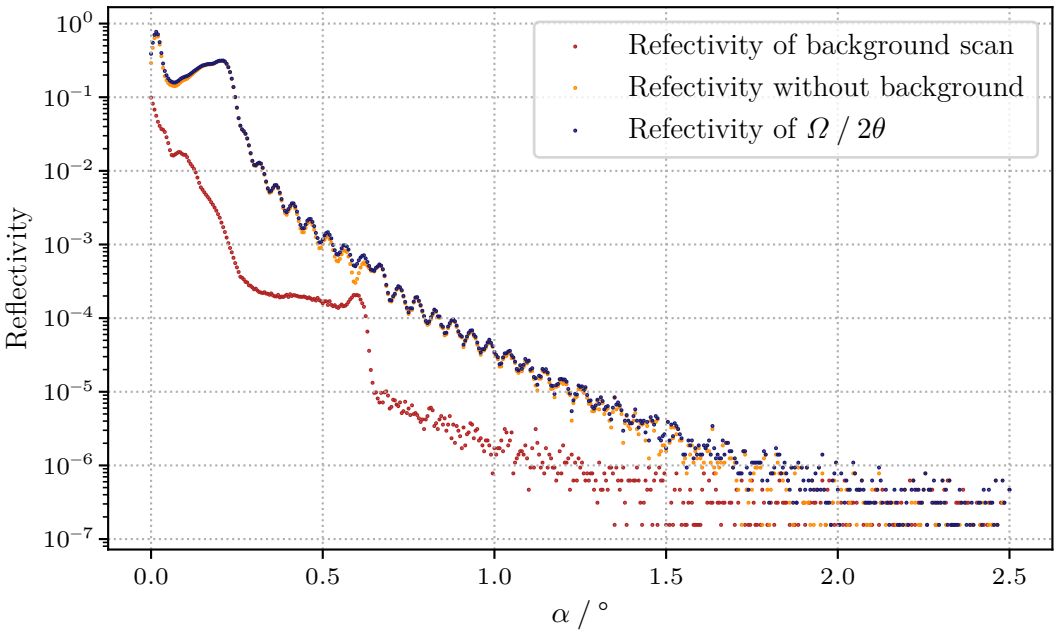

Figure 13: Reflectivity of the two Omega/2Theta scans, where the incidence angle of the diffuse scan is shifted by 0.20°. In addition with the Omega/2Theta, where the diffused scan is subtracted.

The critical angle of Silicon and Polystyrene is calculate with Equation 2 and are

$$\alpha_{\mathrm{Poly,c}} = 0.080\,^\circ \quad \text{and}$$
$$\alpha_{\mathrm{Si,c}} = 0.213\,^\circ .$$

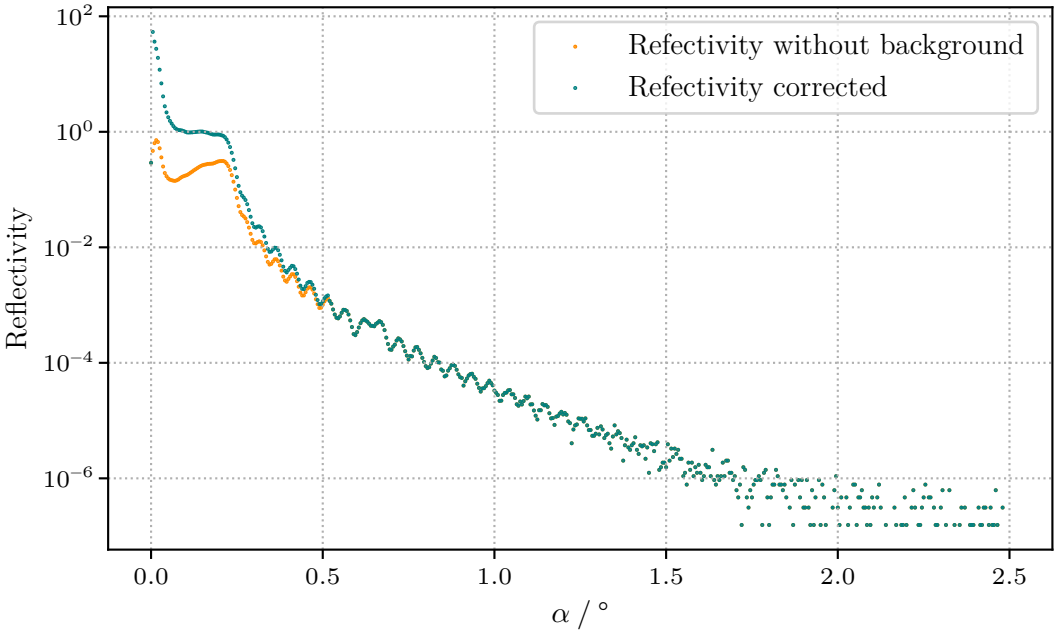

Figure 14: The Omega/2Theta scan with and without the geometry factor correction, and without any background.

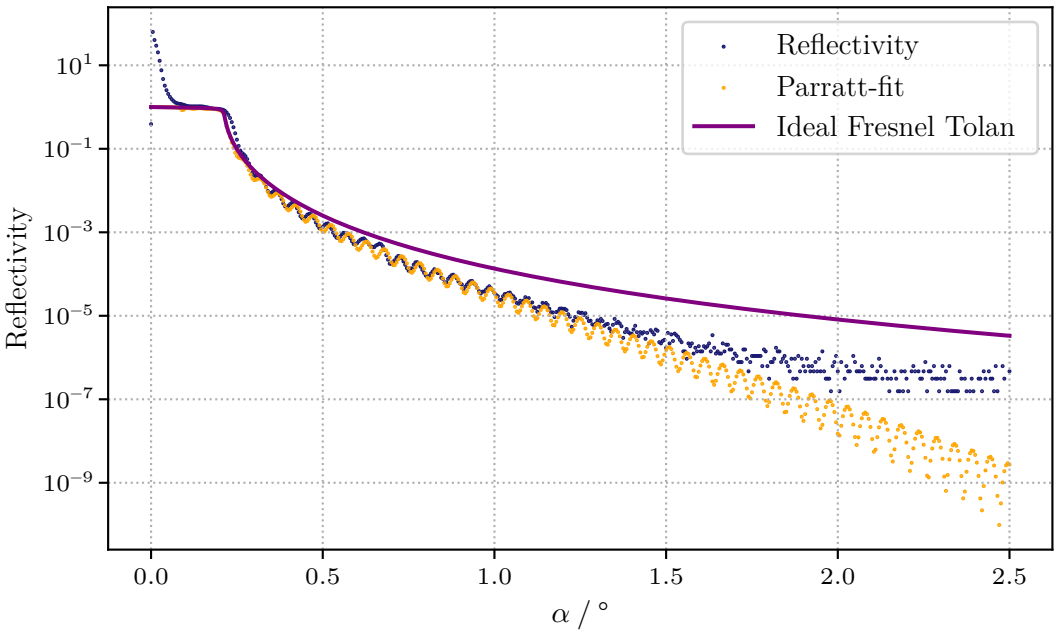

Figure 15: The background-free Omega/2Theta scan corrected by the geometry factor. Alongside the ideal fresnel reflectivity for a smooth silicon surface and the best Parratt-fit.

5 Discussion

The measurement geometry angle is $\alpha_g = (0.520 \pm 0.020)°$ while the theoretical value is $\alpha_{\text{Theo}} = (0.573 \pm 0.057)°$. This results in a relative deviation of $\Delta\alpha = 9.25\,\%$.
The Parratt algorithm delivers $\delta_{\text{Si}} = 6.93 \times 10^{-6}$ and $\delta_{\text{Poly}} = 9.70 \times 10^{-7}$. The literature values are $\delta_{\text{Si, lit}} = 7.60 \times 10^{-6}$ and $\delta_{\text{Poly, lit}} = 3.50 \times 10^{-6}$ [5]. The corresponding relative deviations are $\Delta\delta, \text{Si} = 8.82\%$ and $\Delta\delta, \text{Poly} = 72.29\%$.
Critical angle $\alpha_{\text{Poly,c}} = 0.080\,°$ and $\alpha_{\text{Si,c}} = 0.213\,°$ together with the literature values $\alpha_{\text{Si,theo}} = 0.174\,°$ and $\alpha_{\text{Poly,theo}} = 0.153\,°$. This yields deviations of $\Delta\alpha_{\text{Si,c}} = 22.41\,\%$ and $\Delta\alpha_{\text{Poly,c}} = 47.71\,\%$.
The layer thickness is calculate in two ways giving the values $d_1 = (8.8 \pm 0.7) \times 10^{-8}\,\text{m}$ and $d_2 = 8.49 \times 10^{-8}\,\text{m}$. The deviation of the layer thicknesses is $3.65\,\%$.

The sample might have a scratch, as can be seen in Figure 13. Because the reflectivity has an abnormality at around $\alpha \approx 0.60°$. Most of the calculated values have a high relative deviation from their literature value. This is probably a consequence of a poor fit. Although several methods were tried, no better parameters could be determined. The best agreement is in the layer thickness with $3.65\,\%$, which suggests that the measurement it at least consistent with itself.

References

1. *Practical Gamma-Ray Spectrometry* ISBN: 9780470861981. https://onlinelibrary.wiley.com/doi/book/10.1002/9780470861981 (John Wiley, Ltd, 2008).
2. *Strahlungsquellen für Physik, Technik und Medizin* ISBN: 978-3-662-66746-0. https://onlinelibrary.wiley.com/doi/book/10.1002/9780470861981 (Springer Spektrum Berlin, Heidelberg, 2023).
3. Dresden, T. U. *Röntgenspektrum* ().
4. Tolan, M. *X-Ray Scattering from Soft-Matter Thin Films* (Springer Berlin, Heidelberg, 1999).
5. *V44 X-ray reflectrometry* TU Dortmund, Fakultät Physik (2023).
6. Foundation, P. S. *Python Version 3.8.8* ().
7. Jones, E., Oliphant, T. E., Peterson, P., *et al. SciPy: Open source scientific tools for Python* version 0.16.0. http://www.scipy.org/.
8. Lebigot, E. O. *Uncertainties: a Python package for calculations with uncertainties* version 2.4.6.1. http://pythonhosted.org/uncertainties/.
9. Hunter, J. D. Matplotlib: A 2D Graphics Environment. Version 1.4.3. *Computing in Science & Engineering* **9,** 90–95. http://matplotlib.org/ (2007).
10. Dembinski, H. & et al., P. O. scikit-hep/iminuit. https://doi.org/10.5281/zenodo.3949207 (Dec. 2020).

Appendix

Listing 1: Parrat_Algorithm

```
def Parratt_Algorithmus(angle, delta_poli,
    delta_Si, sigma_poli,
    sigma_Si,beta_poli, beta_si):

  Wellenlänge = 1.54e-10
  k = 2*np.pi / Wellenlänge
  layer_thickness = 8.8e-8
  x_Air_arr = np.zeros(len(angle))
  n_Air = 1
  n_poly = 1 - delta_poli + 1j*beta_poli
  n_Si = 1 - delta_Si + 1j*beta_si

  for i in range(0 , len(angle)):

    k_Air =      k * np.sqrt((n_Air**2 -np.cos(angle[i])**2))
    k_poly =     k * np.sqrt((n_poly**2 -np.cos(angle[i])**2))
    k_Si =       k * np.sqrt((n_Si**2 -np.cos(angle[i])**2))

    r_Air_poly = (k_Air - k_poly)/ (k_Air + k_poly)
      * np.exp(-2*k_Air*k_poly*sigma_poli**2)
    r_poly_Si = (k_poly - k_Si)  / (k_poly + k_Si)
      * np.exp(-2*k_poly*k_Si*sigma_Si**2)

    x_poly = np.exp(-2j * k_poly * layer_thickness) * r_poly_Si
    x_Air = (r_Air_poly + x_poly)/(1 + r_Air_poly  *x_poly)
    x_Air_arr[i] = (np.abs(x_Air))**2

    return x_Air_arr
```